CHAPTER 4

RESULTS AND DISCUSSION FOR CADMIUM SELENIDE (CdSe)

4. RESULTS AND DISCUSSION FOR CADMIUM SELENIDE (CdSe)

In this chapter, the data obtained from the various material characterisation and electrical characterisation techniques for Cadmiumn Selenide (CdSe) is presented and discussed. CdSe has been a widely researched material [80-85] due to its potential for device applications such as solar cells, gamma ray detectors, photoconductors and many more and have been studied closely even up to quantum dot levels. The common methods of preparing this material is by sputtering, vacuum evaporation and electrodeposition. The context of this research utilises mainly the electrodeposition method which was studied comparatively with the electron beam sputtering techniques for solar cell applications.

4.1 Analysis Procedure

The approach to the fabrication and analysis was identical to that described in section 3.1 for CdTe. The same paces were repeated for the setting up stage and variation of various parameters.

4.1.1 Sequence of Events

1. Upon research of literature and obtaining the additional chemicals, the electrochemical bath was set up following the arrangement prescribed is chapter 2. Since a few parameters such as electrode separation and minor changes in the concentration of the individual chemicals of the electrolyte bath were found to have inappreciable differences in the final coated film, these investigative steps were foregone all together. The counter electrode of copper (Cu) was used due to the superior conductivity in the electrodeposition set up and the necessary precautions to avoid diffusion of copper into the sample was taken.

2. The optimisation of the electrodeposition conditions were done by varying the parameters such as deposition time, deposition voltage, continuous stirring and temperature

3. When the desired samples were obtained, they were subjected to verification and characterisation using XRD, EDX, SEM and UV/VIS spectroscopy.

4. The electrical characterisation was done to observe the photovoltaic properties of the n-CdSe/p-Si junction solar cells that were fabricated. This procedure assists in determining the type of silicon that is most useful for solar cell applications and could comparatively show the relative efficiencies of sputtered CdSe as compared to electrodeposited films.

4.2 Electrodeposition of CdSe

The following components of the electrodeposition process, namely the electrodes, electrolyte and the deposition process were studied in greater detail [86] prior to the setting up stage

4.2.1 The Electrolyte

The function of the electrolyte is to provide free ionic mobility of cadmium and selenium ions to form the desired film on the working electrode (cathode). The prescribed salts [87] used as starting materials were $CdSO_4$ (or $CdCl_2$) and SeO_2. CdSe, being a similar II - VI compound as CdTe, would yield a similar voltammogram with only slight changes in the behavioural curves of the component and combined electrolytes.

Once again the cadmium deposition is expected to take place very significantly at 750mV and would experience a large current intensity change due to the higher concentration (0.3M) used. Therefore it is predicted that at voltages exceeding -750mV,

the films would be cadmium rich, which is not what is desired. The much lower concentration of SeO_2 (1 mM), would result in two major waves occuring in the I-V curve. The first wave would be due to $HSeO_2^+$ reduction, leading to a tellurium deposit and the second due to selenium reduction into H_2Se (aq).

From the experience gained in the deposition done on CdTe, it is expected that CdSe would have a codeposition region in the voltage range of -400mV to -750mV. Thus, the deposition voltage was varied in this range and the deposited film was subjected to quantitative (EDX) and qualitative (XRD) studies to determine the formation of CdSe on the films.

The expected global reaction mechanism is as follows :

$$Cd^{2+} + HSeO_2^+ + 3H^+ + 6e^- \rightarrow CdSe + 2H_2O$$

The silicon electrodes cannot be placed in the electrolytic solution as a selenium coating could be formed under open circuit conditions by a corrosion mechanism that can be described in the redox reactions below :

Oxidation mechanism : $Si + 2H_2O \rightarrow SiO_2 + 4H^+ + 4e^-$

Reduction mechanism : $HSeO_2^+ + 4e^- \rightarrow Se + 2H_2O$

The higher tendency of silicon to oxidise requires the precaution whereby the potential is immediately applied to the electrodes as soon as it is immersed in the solution and maintained until the electrodes are removed from the electrolyte.

By cathodic polarization methods described elsewhere [50], where a similar set up of Si-Cu electrodes were used, the most likely potential where the codeposition would take place at a 1:1 ratio is at the voltage of 0.64 - 0.68V

The voltage range of 0.5-0.8V were applied to an electrolyte with the following concentrations:

1. $CdSO_4$ or $CdCl_2$	0.3M
2. SeO_2	0.9mM
3. Ethyl-diamine-tetraacedic acid (EDTA)	15mM

EDTA is used as a complexing agent which reduces the impurities in the salts used by forming complexes in a separate reaction mechanism.

4.2.2 The Electrodes

The working electrode selected for the purpose of coating depositions were five grades of silicon wafers and ITO glass. The depositions on silicon were made for solar cell studies and parellal depositions with identical parameters were deposited on ITO glass as optical characterisation can only be done on transparent samples. These substrate materials were cleaned thoroughly by the procedures described in Chapter 2 and 3. The chosen counter electrode (anode) was copper for the reasons descrided in section 3.2.2.

4.3 The Electrodeposition Process

The electrodes were assembled on an insulating 4cm separator and the necessary electrical connections made. 25ml of the desired electrolyte consisting of $CdSO_4$ (0.3M), SeO_2 (0.9mM) and EDTA (15mM) was prepared. The following variations were applied to the electrodeposition process.

Variations

- The voltage was varied between 500 - 800mV
- The deposition time was varied between 10min - 1 hour
- The effect of stirring the bath was observed
- Five grades of silicon wafers and one grade of ITO were used as working electrodes
- The effects of annealing were studied

These variations were made sequentially to identify the effect of each change. The deposited films have to be thoroughly rinsed in distilled water and dried before subsequent EDX, XRD and electrical characterisation studies (only for determining best silicon grade for solar cell applications)

4.4 Electron Beam Sputtering - CdSe

The steps identical to that described in section 3.4 were taken with the exception of CdSe granules used in place of CdTe. The granules of CdSe were of analar grade and of 99.99% purity.

4.5 Material Characterisation

4.5.1 X-Ray Diffractometry

Once again for the accurate determination of cadmium selenide, diffraction studies were done on CdSe film sputtered on glass and silicon and electrodeposited on silicon and ITO. The film thickness quoted below refer to that obtained from the ensuing optical calculation for thick films (from transmission fringes) and deduction of thickness with respect to time (assuming linearity) for the thin films during sample preparation.

Figure 4.1 shows the diffractogram of CdSe sputtered on silicon as a thin film (4.1a, 300nm) and a thick film (4.1c, 800nm). The diffraction peak is observed at 25.5° corresponding to the theoretical CdSe zinc blend structure. The thicker film has a higher intensity due to a greater material growth on the film. With a larger number of crystallites, the diffraction of the film at a particular angle is larger, resulting in higher intensities. Figure 4.1b and 4.1d show the diffractogram of the same films after annealing at 473K in vacuum for two hours. Higher intensities here are due to the larger grain size as an effect of annealing.

Figure 4.2 shows the diffractogram of CdSe which was sputtered on glass. Once again, a diffraction peak is observed at 25.5°. Figure 4.2a and 4.2c represent the thin and thick CdSe films and 4.2b and 4.2d are the diffractogram of these films after annealing. A similar effect as what was observed for films sputtered on silicon are observed, which enables us to conclude that the substrate (crystalline silicon and amorphous glass) has no consequent on the deposited film.

The diffractograms of CdSe electrodeposited on silicon and ITO glass is shown in Figure 4.3. In 4.3a, no major peaks were observed even though a visible thin coating (≈ 200nm) was formed on silicon. Upon annealing at 473K for two hours in vacuum, a peak corresponding to the CdSe zinc blend phase (25.2°) was observed. A second peak, presumably from cadmium or selenium is also observed. This once again shows that the restructuring of the grain size and gradual phase transitions takes place and annealing is absolutely necessary if highly crystalline films are desired. Figure 4.3c shows the diffractogram of an annealed CdSe film electrodeposited on ITO. Being a thick film (800nm), it displays a strong correspondence to the theoretical peaks for CdSe of the zinc blend structure [88].

Table 4.1 below shows the theoretical peak values for CdSe in the zinc blend structure and the crystalline wurtzite structure[86], as well as the values extracted from figures 4.1, 4.2 and 4.3. By comparing the relative peak intensities, it can be seen that the CdSe films fabricated by electrodeposition and sputtering attain the phase of zinc blend due to the missing major wurtzite peak at 43^0. This confirms accurate depositions.

Table 4.1: Theoretical and Experimentally Obtained Diffraction Peak Values

CdSe Zinc Blend structure (theoretical)			CdSe crystalline wurtzite structure (theoretical)			CdSe sputtered (from fig 4.1 and 4.2)			CdSe electrodeposited (from fig 4.3)		
25.4	(111)	100%	24	(100)	80%	25.5	(111)	100%	25.2	(111)	100%
42.5	(220)	15%	25	(002)	30%						
50	(311)	10%	26	(101)	60%						
			35	(102)	5%						
			43	(110)	100%						
			45	(103)	30%						

Figure 4.1 : XRD of CdSe Sputtered on Silicon

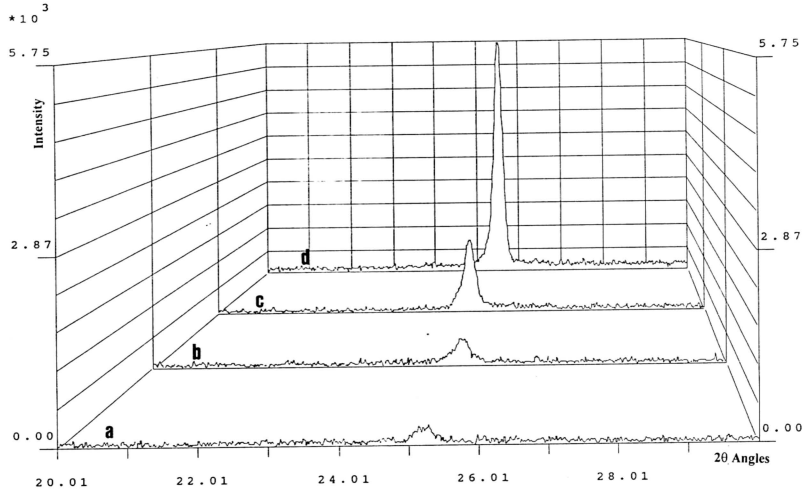

a: Thin Film, b: Thin Film Annealed, c Thick Film, d: Thick Film Annealed

Figure 4.2 : XRD of CdSe Sputtered on Glass

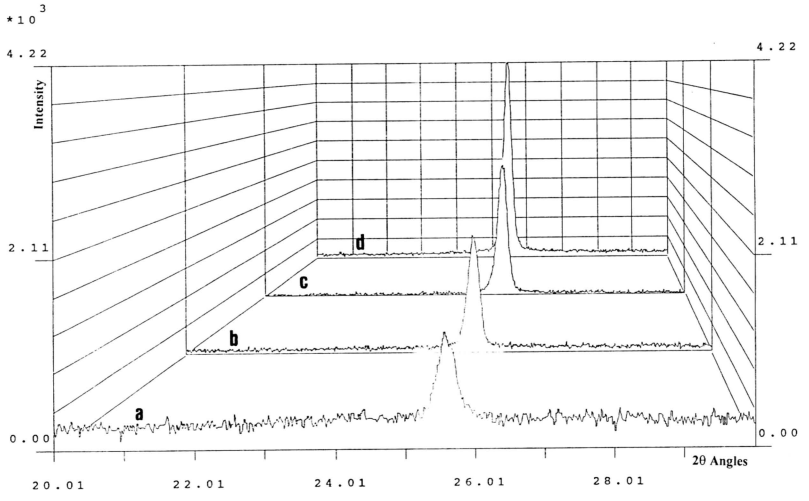

a: Thin Film. b: Thin Film Annealed. c Thick Film. d: Thick Film Annealed

Figure 4.3 : XRD of CdSe Electrodeposited on Silicon and ITO

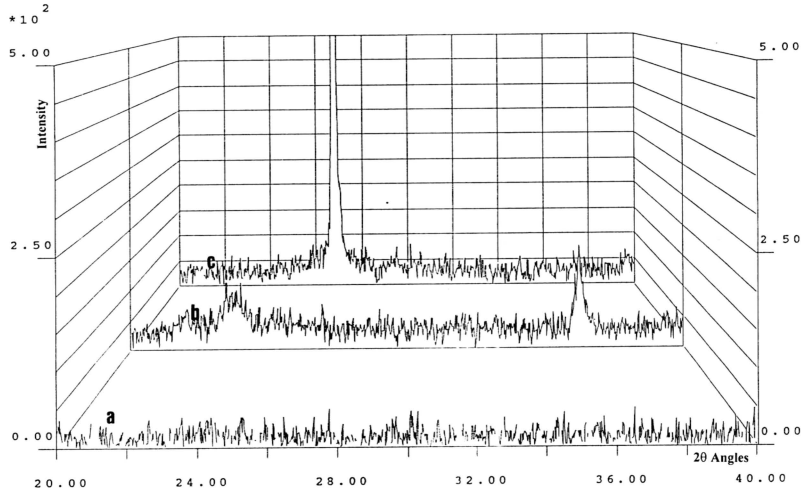

a: Thin Film on Si, b: Thin Film on Si (Annealed), c: Thick Film on ITO (Annealed)

4.5.2 Energy Dispersive Analysis of X-rays

For a quantitative analysis to be more descriptive and better averaged over the entire thin film coated area, the magnification of the SEM is reduced to a level whereby the largest possible area of the film is bombarded by the electron beam. Care was taken to ensure the electron beam is not incident on the uncoated portion of substrate as it would give rise to the silicon counts and give a false inpression that the films are thin.

The most significant EDX spectra in the initial investigation stages regarding deposition voltage and time is presented here. Figure 4.4 (a-c) shows the EDX spectra when the electrodeposition voltage was at 0.5V, 0.65V and 0.8V respectively. The quantification data is presented in the table below.

Table 4.2 The Effect of Deposition Voltage on the Composition of CdSe

Figure	Deposition Voltage (V)	Cadmium (Cd%)	Selenium (Se%)
4.4a	0.50	12.31	87.69
4.4b	0.65	43.81	56.19
4.4c	0.80	62.93	37.07

The quantification data shows that the best deposition is obtained at the voltage of 0.65V as the ratio of cadmium to selenium is closest to 1:1. At lower deposition voltages (<0.6V), the tendency of the deposited film is to be selenium rich whereas at higher voltages (>0.7V), the films were found to be cadmium rich. This closely corresponds to the predictions made based on the voltammogram analysis and the cathodic polarization curve.

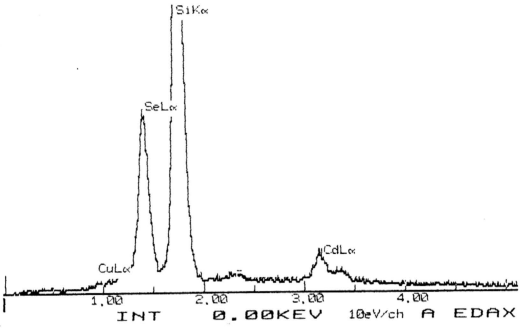

Figure 4.4a : EDX Spectra for CdSe Electrodeposited on Si at 0.5V

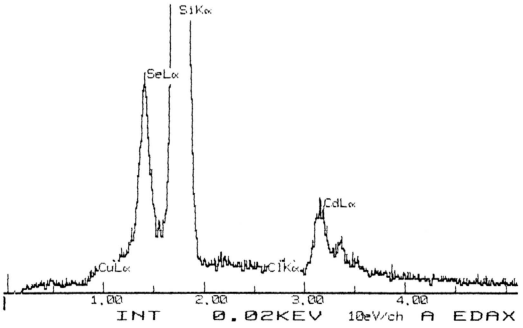

Figure 4.4b : EDX Spectra for CdSe Electrodeposited on Si at 0.65V

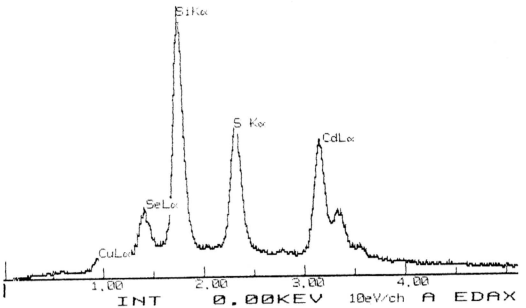

Figure 4.4c : EDX Spectra for CdSe Electrodeposited on Si at 0.8V

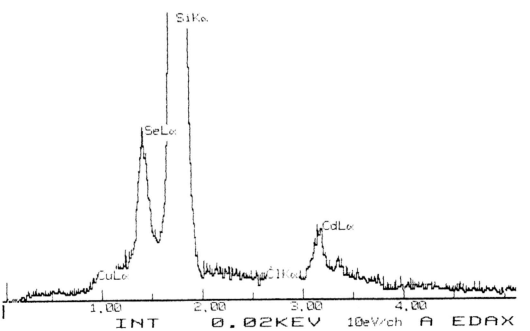

Figure 4.5a : EDX Spectra for CdSe Electrodeposited on Si for 15 minutes (at 0.65V) [Cu electrode exchanged every 5 minutes]

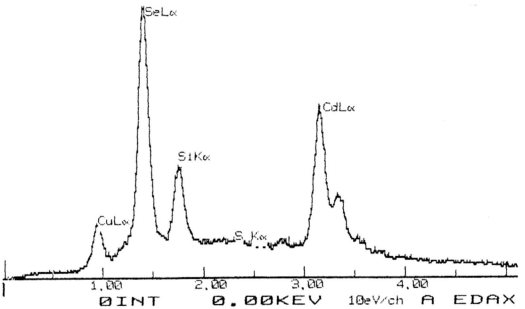

Figure 4.5b : EDX Spectra for CdSe Electrodeposited on Si for 15 minutes (at 0.65V)

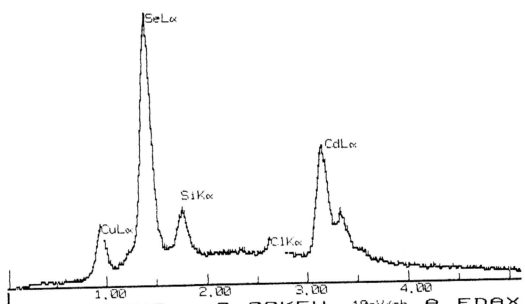

Figure 4.5c : EDX Spectra for CdSe Electrodeposited on Si for 30 minutes (at 0.65V)

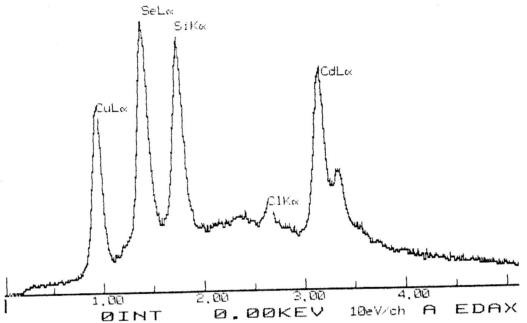

Figure 4.5d : EDX Spectra for CdSe Electrodeposited on Si for 60 minutes (at 0.65V)

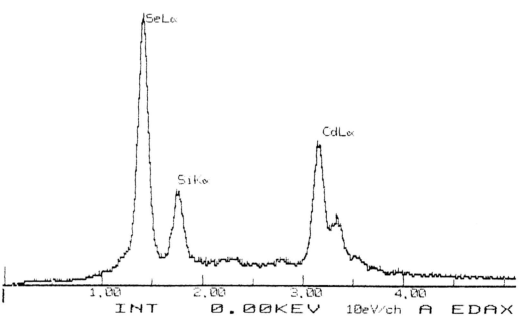

Figure 4.5e : EDX Spectra for CdSe Sputtered on Si

Figure 4.5 (a-d) are presented to show the effect of the deposition time and interchanging the copper counter electrode on the composition of the thin film. All films were deposited at a voltage 0.65V. Figure 4.5a and 4.5b represent a fifteen minutes coating but the copper counter electrode was replaced for 4.5a at five minute intervals. Both these samples showed a high countrate of silicon indicating the coating is generally thin in nature. Figure 4.5c and 4.5d show the spectra for the film obtained after a thirty minutes and sixty minutes deposition time with no electrode replacement. The quantification data is tabulated below. Additionally, Figure 4.5e shows the EDX spectra for a silicon substrate sputtered with CdSe and later quantified.

Table 4.3 The Effect of Deposition Time on Composition and Relative Thickness

Figure	Deposition Time (minutes)	Comparative Thickness	Cadmium (Cd%)	Selenium (Se%)
4.5a	15	Thin	47.57	52.43
4.5b	15	Thin	39.41	60.59
4.5c	30	Medium	43.98	56.02
4.5d	60	Thick	54.44	45.56
4.5e	Sputtered	Thin	44.22	55.78

All the spectra in figure 4.5(b-d) indicated a presence of copper presumably from the counter electrode. When the copper electrode was replaced at five minutes intervals as seen in figure 4.5a, no presence of copper was detected. This proves the advantage of copper electrode replacement. The trend that deposition thickness increases with time can be seen as a progressive reduction on silicon intensities with longer deposition times. The sputtered film (figure 4.5e) displayed a 1:1 ratio of cadmium and selenium reflecting good stoichiometry. This is an expected outcome as CdSe granules of 99.99% purity was used as the starting material.

The information on thickness and composition was used to optimise the deposition voltage and time and supported the advantage of copper electrode replacement periodically during the electrodeposition process.

4.5.3 Scanning Electron Microscopy (SEM)

The surface morphology and average grain size is evaluated using micrographs obtained from the scanning electron microscope (SEM). The samples chosen for this purpose are CdSe thin films sputtered on silicon, electrodeposited on silicon and electrodeposited on conducting ITO glass. The interesting features of this film were revealed at magnifications ranging from 5000X to 30000X. Six of the most informative and clear micrographs (in terms of resolution) were chosen to be presented here.

Figure 4.6a and 4.6b are micrographs of CdSe sputtered on silicon at 10000X and 15000X magnification respectively. Apart from a few surface deformities, the thin CdSe films were found to have an extremely uniform grain distribution with very small particle sizes. The micrograph at 15000X could not reveal the average grain size but it is estimated to be <0.1μm.

The micrographs of CdSe electrodeposited on silicon are shown in Figure 4.7a and 4.7b at magnifications of 10000X and 15000X respectively. The polycrystalline nature of the material can be clearly observed by the particulate distributions. The 10000X magnification micrograph also shows a typical grain distribution of an electrodeposited film with a certain level of porosity, but an equal and uniform grain distribution. The surface particles of light contrast and the bulk particle of dark contrast can be distinguished clearly and micropores are observed in the inter grain locations. The average grain size is measured on micrograph 4.7b and is estimated to be about 0.1-0.3μm.

Micrographs of CdSe electrodeposited on ITO are shown in Figure 4.8a and 4.8b. An interesting feature noted on these micrographs is that the grain size was found to be a little larger than that deposited on silicon. The average grain size is approximated to be in the 0.2 - 4μm range as observed from the 20000X magnification micrograph. Due to the larger average particle size, the film appears to be more porous than 4.7a and 4.7b. This can only be explained as the effect of the substrate conductivity and substrate

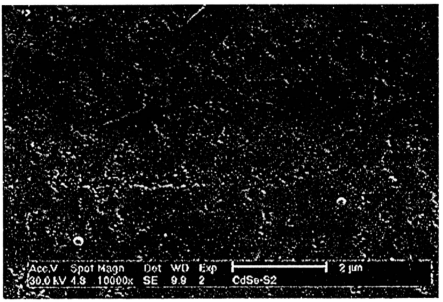

Figure 4.6a : Micrograph of CdSe Thin Film Sputtered on Silicon (10000X)

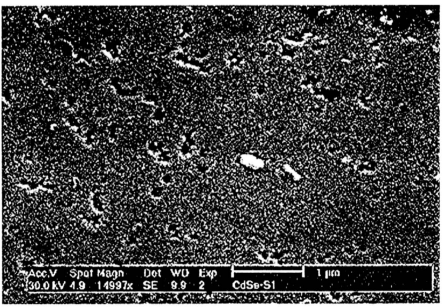

Figure 4.6b : Micrograph of CdSe Thin Film Sputtered on Silicon (15000X)

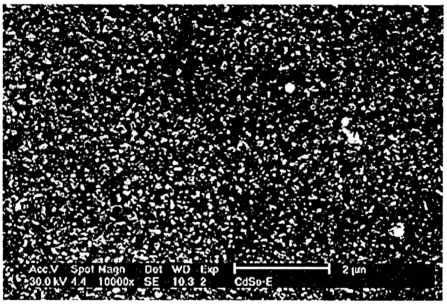

Figure 4.7a : Micrograph of CdSe Thin Film Electrodeposited on Silicon (10000X)

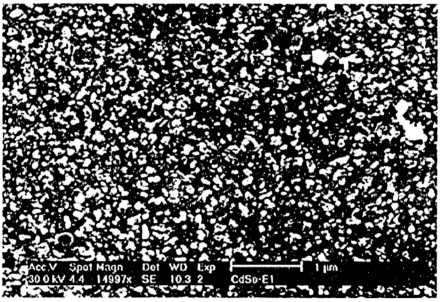

Figure 4.7b : Micrograph of CdSe Thin Film Electrodeposited on Silicon (15000X)

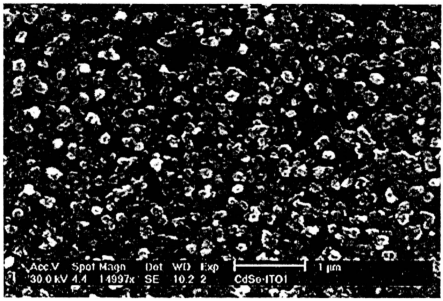

Figure 4.8a : Micrograph of CdSe Thin Film Electrodeposited on ITO (15000X)

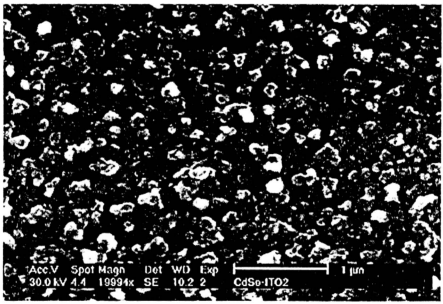

Figure 4.8 b : Micrograph of CdSe Thin Film Electrodeposited on ITO (20000X)

surface structure on the deposited film. All other electrodeposition parameters were maintained in a similar manner as when deposition on silicon was done.

4.5.4 UV-Visible Spectrometry

The optical characterisation of CdSe was obtained from the absorption and transmission spectra of the films coated on transparent substrates. The transparent substrates used were glass for sputtered CdSe and ITO glass for electrodeposited CdSe.

For the thicker films, the transmission fringes enable the calculation of the refractive index (n), absorption coefficient (α) and film thickness (t) using the envelope method as prescribed in section 3.3.4. Following this, a plot of $(\alpha hf)^2$ versus energy (hf) is plotted and the intercept of the extrapolation of the absorption edge with the x-axis would yield the value of the energy gap.

For the thinner films, the absorption spectra is used to obtain the energy gap since no significant transmission fringes are apparent. This is done by extrapolating the absorption edge to the energy axis. This method yields a good approximation of the energy gap (E_g) and can be compared with the calculations of E_g from the transmission spectra and theoretical values for confirmation.

Figure 4.9 shows the transmission spectra for the transparent sputtered and electrodeposited CdSe thin films. The method how the transmission spectra is fitted for the envelope method is shown in figure 4.10 for extraction of the values λ_1, λ_2, $T_{\lambda 1\ max}$, $T_{\lambda 1\ min}$, $T_{\lambda 2\ max}$ and $T_{\lambda 2\ min}$ to be used in the calculations in the envelope method. In figure 4.9, the trend that can be noted is that the occurrence of more interference fringes can be observed for the thicker samples. The thinner samples display almost no fringes and resemble a straight line in some cases. The plot for $(\alpha hf)^2$ versus energy (hf) and the extrapolation to obtain the energy gap is shown in figure 4.11.

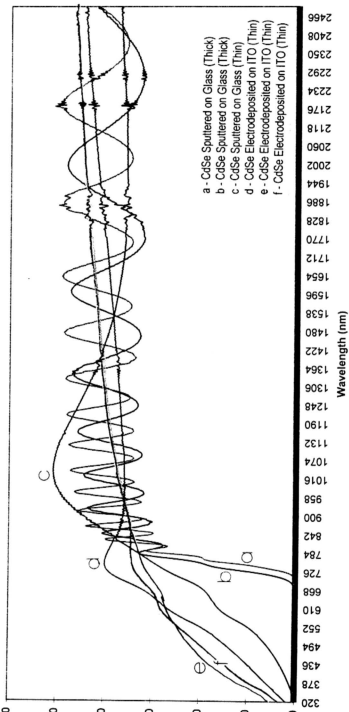

Figure 4.9 : Transmission Spectra (T%) of CdSe Sputtered on Glass and Electrodeposited on ITO

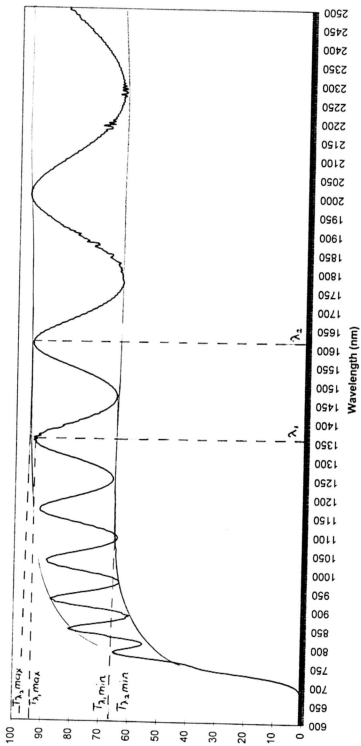

Figure 4.10 : Transmission Spectra of CdSe Sputtered on Glass (Showing fitting for the envelope method)

Figure 4.11 : $(\alpha hf)^2$ vs. Energy - Extrapolated to obtain Energy Gap

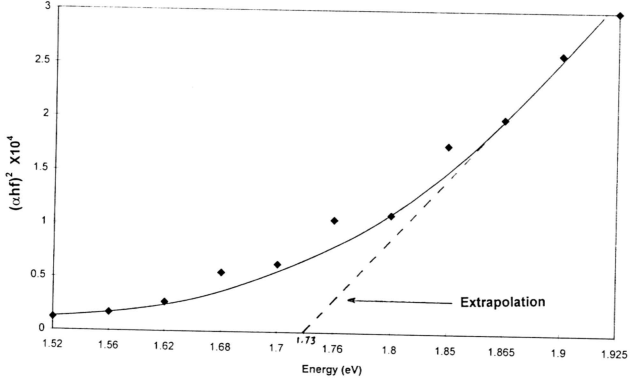

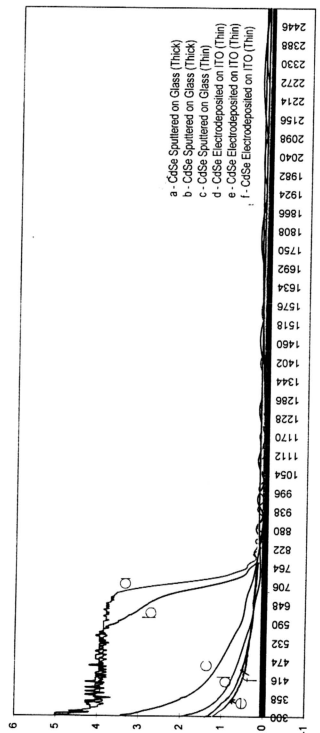

Figure 4.12 : Absorption Spectra of CdSe Sputtered on Glass and Electrodeposited on ITO

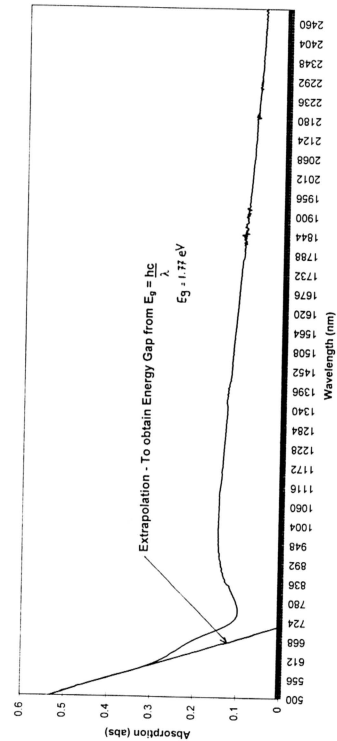

Figure 4.13 : Absorption Spectra of CdSe Electrodeposited on ITO

Figure 4.12 shows the absorption spectra for the same series of samples as the transmission spectra above. It can be seen that even though the absorption edge varies from sample to sample, the point of intersection to the x-axis is in the range of 700nm - 800nm. This is in close agreement with theoretical values as the wavelength corresponding to the energy gap (from $E\lambda=hc$) of the material is in this region. The absorption edge extrapolation from an absorption spectra of the thin sample is shown in Figure 4.13. This method is repeated for all thin samples for computation of the energy gap.

The outcome of the calculations can be tabulated and compared with theoretical values in the table below.

Table 4.4: The Theoretical Values and the Calculated Values of Various Optical Parameters

Sample	Theoretical refractive index*	Calculated refractive index*	Theoretical energy gap (eV)	Calculated energy gap (eV)	Calculated thickness (nm)
CdSe Sputtered - Glass (Thick)	2.75	2.80	1.74 eV	1.80	1703
CdSe Sputtered - Glass (Thin)	2.75	2.66	1.74 eV	1.73	863
CdSe Electrodeposited - ITO (Thick)	2.75	2.85	1.74 eV	1.81	1194
CdSe Electrodeposited - ITO (Medium)	2.75	2.78	1.74 eV	1.77	765
CdSe Electrodeposited - on ITO (Thin)	2.75	-	1.74 eV	1.68	$\pm$ 400

* Theoretical values attained from [79]

4.6 Electrical Characterisation

4.6.1 Open Circuit Voltage (OCV) and Short Circuit Current (I_{SC})

The purpose of electrical characterisation of the deposited samples was to study the effectiveness of the respective n-CdSe/p-Si junction to function as photovoltaic converters. The first stage of analysis is to purely investigate the open circuit voltage (OCV) and short circuit current (I_{SC}). This experiment was carried out with the five grades of silicon wafer used (Type I-V). Thin CdSe films of approximate thickness of 600nm, were electrodeposited on these five wafer types. The outcome of the OCV and I_{SC} upon illumination as described in section 2.5 is tabulated below.

Table 4.5: The OCV and I_{SC} for CdSE Thin Films on Various Silicon Grades

Wafer Type	OCV (Measured mV)	Resistance (kΩ) (Measured)	Short Circuit Current, (I_{SC}) (Calculated)
Type I	0	110 kΩ	-
Type II	210	160 kΩ	1.93 μA
Type III	20	120 kΩ	0.16 μA
Type IV	85	110 kΩ	0.72μA
Type V	260	130 kΩ	2 μA

The trend that is seen here is as observed in section 3.6, where the best solar characteristics are obtained from the type II and V grade silicon wafer as the resistivity of these grades of wafers fall within the recommended range of 5-100Ωcm^{-1} for photovoltaic activity. Type III and IV wafers displayed very low and negligible solar activity due to the very low resistivity. The type I wafers (p-type) did not show any photovoltaic activity due to the lack of a p-n junction formation.

A similar analysis step as mentioned above is done for the purpose of comparing the photovoltaic activity of thick and thin electrodeposited CdSe films on type V silicon as opposed to a sputtered CdSe thin film on type V silicon. The resulting OCV and I_{SC} data is tabulated below for comparison purposes.

Table 4.6: The Comparative OCV and I_{SC} for Sputtered and Electrodeposited CdSe Thin Films

Wafer Type	OCV (Measured)	Resistance (kΩ) (Measured)	Short Circuit Current, (I_{SC}) (Calculated)
Sputtered	275	125 kΩ	2.2 μA
Electrodeposited CdSe (Thin)	260	130 kΩ	2 μA
Electrodeposited CdSe (Thick)	250	147 kΩ	1.5 μA

4.6.2 Current-Voltage (I-V) Characteristic Curve

The I-V characteristic curve is constructed by measuring the external circuit current and incident voltage across the cell when a varying external load is applied. The circuit connection and conditions for consistent illumination area and intensity is as described in section 2.5

Figure 4.14 shows the I-V curve of the same three films that were analysed for OCV and I_{SC} characteristics in Table 4.6. Additionally, the plot of a theoretical ideal curve where no losses are observed due to series resistance $R_S = 0$ and shunt resistance $R_{SH} \rightarrow \infty$ is also shown. The series resistance has the effect of reducing the I_{SC} and affects the OCV adversely.

It is observed that the sputtered film had the highest OCV and I_{SC}. The comparison of the thick and thin electrodeposited films clearly shows that a thin film is more favourable for solar cell application from the shape of its individual I-V curve. The reason behind the poorer solar performance of the thicker film is that more light energy is lost in the absorption within the film and also because of higher resistance of the thicker film and thus the lower I_{SC}.

The sputtered film, due to its lower porosity, has lesser losses due to shunt resistance as the possibility of electron leakages is less compared to the porous electrodeposited samples. The losses in power of the solar cell can be noted by the drift of the I-V characteristic curve away from the ideal curve due to series resistance (reduced I_{SC}) and shunt resistance (reduced OCV).

It can thus be concluded from figure 4.14 that the sputtered CdSe film has a marginally better performance than the electrodeposited thin film. However, the electrodeposition method was practically found to be easier and less time consuming than the sputtering technique.

Figure 4.14 : I-V Characteristic Curve of CdSe Sputtered on Si and Electrodeposited on Si